
Article:
Zhang, J., Nanayakkara, K.I., He, L. et al. (2026) Digital design optimization and off-site modularization for modern stone masonry construction. Engineering Structures, 353, Part C. 122349. ISSN: 0141-0296

https://doi.org/10.1016/j.engstruct.2026.122349

Digital Design Optimization and Off-Site Modularization for Modern Stone Masonry Construction

Jian Zhang[a,b], Kavinda Isuru Nanayakkara[b], Linwei He[b,*], Helen Fairclough[b], Andrew Liew[c], Colin Smith[b], Matthew Gilbert[b,†]

[a] *Key Laboratory of Structural Dynamics of Liaoning Province, College of Sciences, Northeastern University, Shenyang, 110819, China*
[b] *School of Mechanical, Aerospace and Civil Engineering, The University of Sheffield, Mappin Street, Sheffield, S1 4DT, South Yorkshire, UK*
[c] *Unipart Construction Technologies, Advanced Manufacturing Park, Rotherham, S60 5WG, South Yorkshire, UK*

Abstract

This research presents an optimization-driven computational design and fabrication method for off-site construction (OSC) of unreinforced masonry structures. Aimed at modernizing sustainable stone construction, this work first introduces a parametric design model that automates the geometry generation and structural analysis of such structures. A key innovation is the application of truss layout optimization to design a reusable support cassette for holding and transporting pre-assembled stone arches. Furthermore, through controlled laboratory replication of on-site assembly, the structural behaviour during the critical lifting and placement phases was closely monitored, revealing the constructed arch's inherent strength and stability. The optimized truss-like cassette system demonstrated satisfactory performance, with adjustable components effectively securing arch blocks for precise fit, aided by careful fabrication tolerances and laser-cut precision. The inter-block gaps are effectively minimised via either turnbuckles or ratchet straps. Simple assembly experiments underscore the significant potential of OSC to enhance the efficiency of unreinforced masonry construction. The challenges in the design and setup process have been reported and evaluated to provide insights

*Corresponding author. Email: linwei.he@sheffield.ac.uk
†Deceased.

for future work. This study solidifies the effective integration of computational design and digital manufacturing, significantly advancing modern OSC and streamlining sustainable building practices.
Keywords:

Digital design, Off-site construction, Unreinforced masonry structures, Truss layout optimization, Cassette design, Pre-assembled arch

---

1. Introduction

The longstanding tradition of stone masonry in construction is underpinned by the material's favorable performance characteristics, where its intrinsic properties and capacity for forming stable compressive structures result in notable durability and aesthetic value [1]. The inherent durability of stone provides high resistance to weathering, fire, and decay, resulting in exceptional longevity and minimal maintenance requirements compared to materials like steel or timber [2]. Furthermore, the substantial thermal mass of masonry can enhance a building's energy efficiency [3], while the arch form efficiently channels gravitational loads through compression, ensuring inherent stability. Despite the desirable properties of the stone masonry, the widespread reintegration of stone into modern building practices faces significant challenges. Traditional masonry construction is often characterized as labor-intensive, time-consuming, and dependent on specialized craftsmanship [4]. This reliance on skilled labor and manual processes stands in stark contrast to modern construction methods, which prioritize efficiency through prefabrication, modularization, and automation [5, 6]. Although the discrete components of masonry structures, such as arches and individual blocks, appear amenable to modular construction, ensuring stability during intermediate on-site construction phases presents a significant challenge. For example, traditional arch construction typically involves the use of temporary formwork (falsework) until the arch achieves its final geometry, including the placement of the keystone and the supporting

abutments. This inherent requirement for full geometric completion before structural integrity is achieved poses a key obstacle to the implementation of modular and prefabricated masonry systems.

Off-site construction (OSC), characterized by the fabrication of building components or modules in a controlled factory environment [7, 8, 9], has become a prominent modern construction method. OSC approach streamlines construction, offering advantages over traditional on-site methods [10, 11], including increased efficiency and speed [12], improved sustainability [13], and enhanced safety [14]. These prefabricated elements, ranging from individual components like walls and floor panels to complete volumetric modules such as fully-fitted rooms, are then transported to the construction site for final assembly [15]. OSC encompasses varying levels of prefabrication, determined by when the final geometry of a structural element is achieved [16]. At the lowest level, individual blocks for an arch might be transported to site, with the arch geometry realized during on-site assembly, similar to traditional arch construction using falsework (although modern techniques employing cooperating robots offer a scaffold-free alternative [17]). The 'FlexiArch' system represents a higher level of prefabrication, where concrete blocks are flexibly connected at the extrados off-site, allowing the arch to assume its final geometry upon lifting [18]. The highest level involves complete off-site fabrication, such as a prestressed stone column and the prefabricated trussed rafter roof [19]. This spectrum of prefabrication levels directly influences the complexity of the subsequent on-site assembly and the temporary support required to facilitate it.

A key factor often underestimated in the efficiency of OSC is the need for temporary support structures. Although some pre-fabricated units are designed as self-supporting "final-form" systems [20], many others require external bracing to maintain stability until final connections are made. The design and implementation of these temporary systems are a significant focus of OSC research. For instance, simulation-driven approaches have been used to redesign wood framing supports, resulting in systems

that are more cost-effective and productive [21]. In more unconventional applications, the successful transport of a massive, fully prefabricated building required a custom truss-like transition structure to provide support during its journey [22]. Similarly, the standard practice for securing precast concrete wall panels involves diagonal steel braces tied to the floor slabs, which are removed only after the permanent structure provides lateral stability [23].

The increasing adoption of parametric and building information models within the construction industry is driving the integration of computational tools for enhanced design and construction processes [24]. These digital tools have facilitated the development of innovative and complex architectural designs [25]. Beyond enabling the creation of unique forms, computational design also supports the prefabrication of building components and systems, streamlining construction workflows. This is particularly beneficial for off-site modularization, where the application of computational design is becoming increasingly prevalent [26]. Accurate computational analysis and real-time visualization are crucial for understanding masonry structures, necessitating sophisticated modeling strategies that can capture their complex, non-linear behavior [27]. In response, the field has developed a diverse range of advanced digital tools and workflows. These innovations often focus on automating and streamlining the modeling process. For instance, image-based and scan-to-FEM approaches automate geometry generation: one framework extracts geometrical features directly from images for advanced numerical analysis [28, 29], while a parametric scan-to-FEM approach transforms point clouds into detailed finite element models for historic structures [30]. A methodology is proposed for the load-bearing capacity assessment of arch bridges, integrating defects identified through visual inspection into a 2D rigid-block limit analysis [31]. Further advancing automation, convolutional neural networks have been introduced to directly detect masonry units and cracks in images [32]. Recently, the PoliBrick plugin for Rhino/Grasshopper enables the parametric digital modeling of intricate brick patterns

on diverse geometries, from flat walls to complex shells [33]. Alongside automation, significant research has developed hybrid and multi-step analytical strategies to balance computational efficiency with accuracy. For instance, a CAD-interfaced tool that links Rhino for drawings with MATLAB for nonlinear dynamic collapse analysis [34]. A two-step procedure for dry-joint structures that first identifies failure mechanisms via limit analysis and then automatically creates a concurrent 3D FE model, coupling micro- and macro-modeling [35]. A hybrid strategy that synergizes the computational speed of Monte Carlo simulation with the accuracy of mechanics-based finite element modeling for estimating out-of-plane resistance [36]. The critical goal is to achieve accurate, real-time simulation of structural behavior, thereby unlocking the benefits of OSC for masonry. While OSC is well-established for materials like concrete [37], steel [38, 39], and wood [40], its potential to revolutionize the traditionally on-site and labor-intensive practice of stone masonry remains largely unexplored. The development of robust digital tools, as summarized here, is a fundamental prerequisite for unlocking this potential.

This paper investigates the integration of computational design and OSC technologies to address inherent limitations in traditional unreinforced stone masonry construction. Through this integration, the research spans digital design, off-site fabrication, transportation, and critical performance demonstration, refer to Figure 1. A comprehensive computational framework is presented, encompassing parametric design, limit analysis, and a novel reusable cassette system designed for the efficient assembly of prefabricated stone elements [41, 42]. This framework specifically applies truss layout optimization algorithms to design a robust structural cassette system enabling the preassembly of stone arches. Components of the cassette derived from numerical design are then precisely fabricated using advanced manufacturing techniques, notably laser cutting. Critically, experimental testing of a scaled masonry structure validated the feasibility of our modern construction approach. Results confirmed the cassette frame's

safety and stiffness, demonstrating the efficient assembly of prefabricated stone arch sections. While our numerical model predicted overall structural stability, the experimental setup revealed challenges with the supporting structure, specifically the column and buttress connections. Additionally, the limited contact area at the springer-arch interface, likely due to non-flat surfaces and positioning inaccuracies, warrants further investigation, especially considering the absence of mortar in this study. Furthermore, we successfully demonstrated a safe cassette removal procedure, though further research is needed for full-scale scenarios where under-arch access is limited. Despite areas for improvement, this research, by combining advanced digital design tools with physical testing, establishes innovative and validated OSC approaches for unreinforced stone masonry, thereby revitalizing this sustainable and historically significant building material for contemporary use.

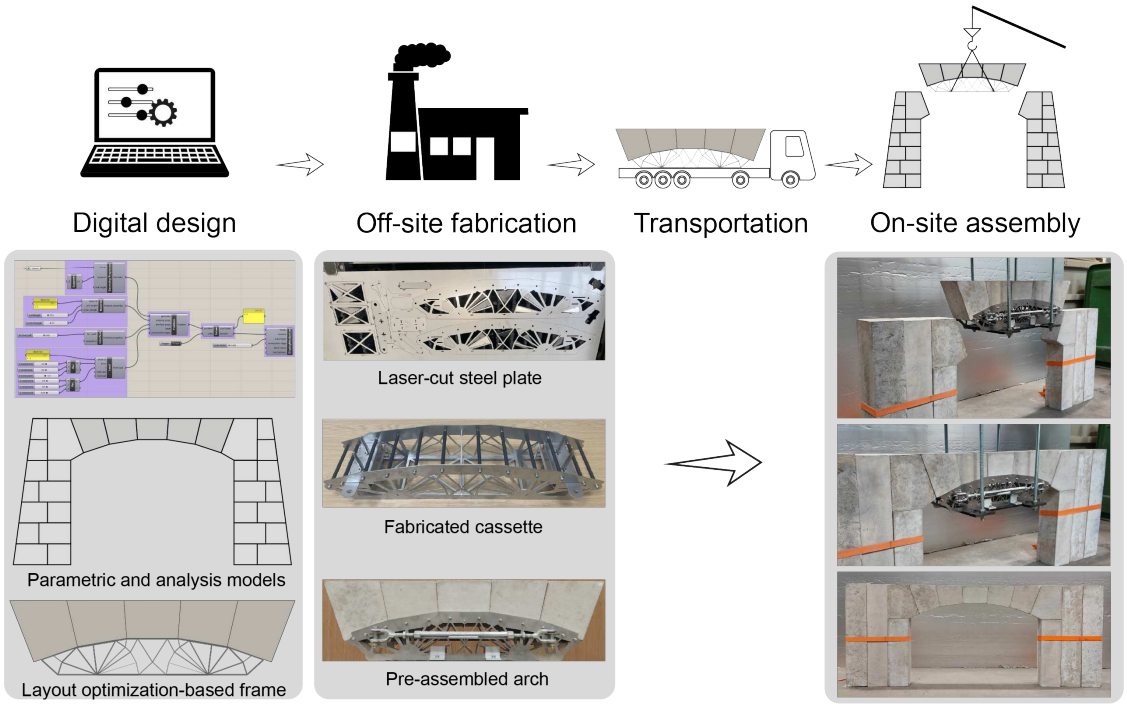

Figure 1: Key stages of the proposed modern stone masonry construction framework: digital design, off-site fabrication, transportation, and on-site assembly.

2. Digital Design

A comprehensive computational model implemented within the Rhinoceros & Grasshopper platform is developed for the design, analysis and off-site construction of unreinforced stone masonry structures. This digital model comprises three interdependent modules: a parametric modelling module facilitating complex form generation, a structural analysis module enabling performance evaluation, and a cassette frame design module specifically tailored for off-site fabrication processes. Crucially, these components do not operate in isolation but constitute a continuous digital thread; geometric parameters and structural data serve as the primary generative drivers for off-site fabrication logic. By retaining the modeling and analysis phases within the core workflow, the integrity of the structural data is preserved throughout the transition to cassette design. This holistic integration eliminates the data loss typical of fragmented design-to-production pipelines, fostering innovation and efficiency in the application of stone as a high-performance modern material.

2.1. Parametric model

To demonstrate the capabilities of the proposed parametric model, a simplified stone masonry building with a rectangular footprint is analyzed. The structural system consists of a network of stone columns, arches, and buttresses, which can be extended to include stone vaults for floor support. The model is developed in Rhinoceros using the Grasshopper visual scripting environment, enabling the manipulation of key design variables through an intuitive interface. These variables (illustrated in Figure 2) are categorized as follows:

- Topological parameters: Number of bays (n_b) and floors (n_f).
- Geometric parameters: Dimensions of individual elements, including column width (t_c), height (h_c), and thickness (d_c), arch span (s), arch rise (r), arch stereotomy

parameter (a), minimum arch height (h_{min}), buttress widths ($t_{\mathrm{b,t}}$ and $t_{\mathrm{b,b}}$), and stagger (t_{s}).

- Discretization parameters: The number of blocks used to construct arches ($n_{\mathrm{b,a}}$) and columns ($n_{\mathrm{b,c}}$).

All parameters serve as manual inputs, allowing designers to rapidly generate and evaluate a wide range of unreinforced masonry structures.

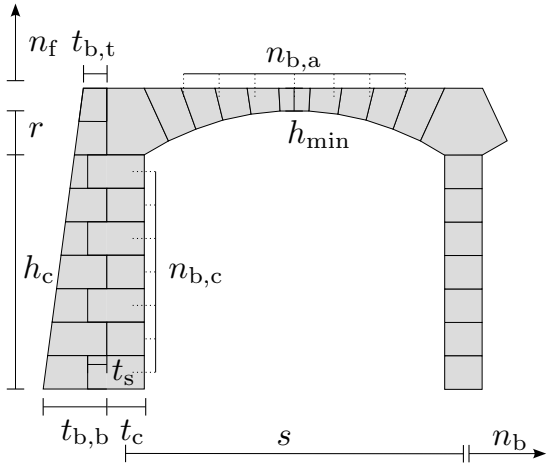

Figure 2: Parametric variables defining the structural topology and geometry of a masonry model, including the number of bays (n_{b}), floors (n_{f}), column width (t_{c}), column height (h_{c}), arch span (s), arch rise (r), minimum arch height (h_{min}), buttress widths ($t_{\mathrm{b,t}}$, $t_{\mathrm{b,b}}$), stagger (t_{s}), and the number of blocks of arches ($n_{\mathrm{b,a}}$) and columns ($n_{\mathrm{b,c}}$).

The generative procedure for the parametric masonry structure follows a sequential, hierarchical workflow, progressing from one-dimensional guide geometry to three-dimensional volumetric blocks, and culminating in a complete global assembly. The process begins by constructing a wireframe defining the structural skeleton, which is then subdivided into discrete, constructible blocks. These elements are subsequently transformed from two-dimensional cross-sections into solid three-dimensional volumes. Finally, the individual components are replicated and assembled into the full building structure. This procedural pipeline is detailed in the following sections.

Phase 1: Definition of Base Guide Geometry

- **Column Layout:** Centerlines for stone columns are established. Their positioning is determined by the topological parameters, specifically the number of bays (n_{b}), which dictates the grid spacing along the building's footprint.

- **Arch Profiling:** The intrados and extrados of the arches are generated. These critical curves are parametrically defined by the arch span (s), arch rise (r), and minimum arch height ($h_{\min}$). The specific curvature (e.g., circular, pointed) is controlled by the stereotomy parameter (a), allowing for design-driven variations in arch geometry.

Phase 2: Discretization into Individual Blocks

- **Segmentation:** The previously created arch curves and column centerlines are divided into a specified number of segments. This is controlled by the number of arch blocks ($n_{\mathrm{b,a}}$) and column blocks ($n_{\mathrm{b,c}}$) parameters, directly influencing the granularity and scale of the masonry work.

- **Cross-Section Generation:** At the division points along each segment, the block's cross-section is defined. For each block, a list of four corner points is calculated, representing a quadrilateral profile. The dimensions of this profile are derived from geometric parameters like the column width (t_{c}) and the buttress widths ($t_{\mathrm{b,t}}, t_{\mathrm{b,b}}$).

Phase 3: Volumetric Extrusion of Masonry Elements

- **Extrusion:** Each quadrilateral cross-section is extruded along its local axis to generate a solid block. The thickness parameter dictates the depth of this extrusion, giving volume to the arches, columns, and buttresses. This step finalizes the creation of fundamental building units: arch voussoirs, column blocks, and buttress stones. To enhance structural stability, the stagger parameter (t_{s}) is used to

strategically offset columns and buttresses, effectively interlocking the structure and increasing its overall robustness.

Phase 4: Global Assembly and Replication

- **Spatial Replication:** Using the topological parameters for the number of floors (n_{f}) and number of bays (n_{b}), the process defined in Phases 1–3 is systematically repeated and spatially arrayed.

The parametric model employs a hierarchical procedure, progressing from initial guide curves through cross-sections and volumes to a global assembly, to efficiently generate a complete and detailed 3D model of an unreinforced masonry structure from a defined set of inputs. This framework enables designers to rapidly explore a wide design space while maintaining architectural and structural validity. A flow diagram illustrating this procedural hierarchy and the resulting geometric model are presented in Figure 3. The resulting geometry provides the topological data necessary for the subsequent structural evaluation.

2.2. Structural analysis

To ensure structural integrity, the parametric model is directly linked to a 3D limit analysis model implemented in LimitState:RING software [43]. This software idealizes masonry structures as assemblages of rigid blocks and employs a concave contact formulation with an iterative solution procedure to solve the non-associative friction problems [44], thereby determining the ultimate limit state and the live load capacity at collapse. The integration of analysis within the parametric design environment, achieved through a suite of custom Grasshopper components, streamlines the structural design process by enabling rapid assessment and iterative refinement. The architecture of this integrated system is depicted in Figure 4, while Table 1 enumerates the names and functions of its constituent components. These custom components form a seamless pipeline, transferring data from the parametric model to the analysis engine.

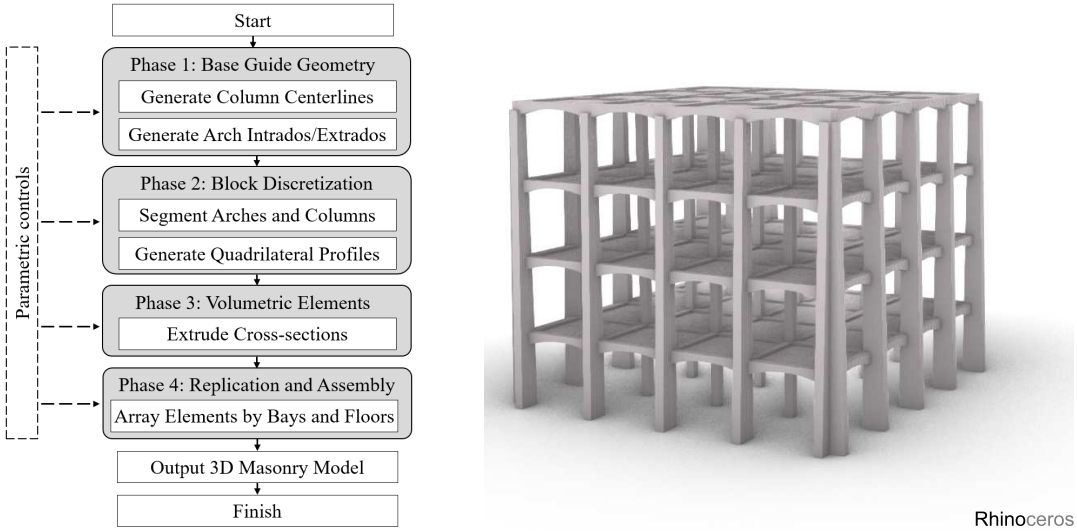

(a) (b)

Figure 3: Parametric modeling framework for masonry structures: (a) Generative workflow diagram illustrating the procedural hierarchy. Visual styling color-codes the components: user-defined parameters (dashed outline, white background), automated algorithmic components (solid outline, white background), and major procedural phases (grey background). (b) Resulting geometric model visualized within the Rhino environment with parameters $n_{\mathrm{f}} = 4$ and $n_{\mathrm{b}} = 4$.

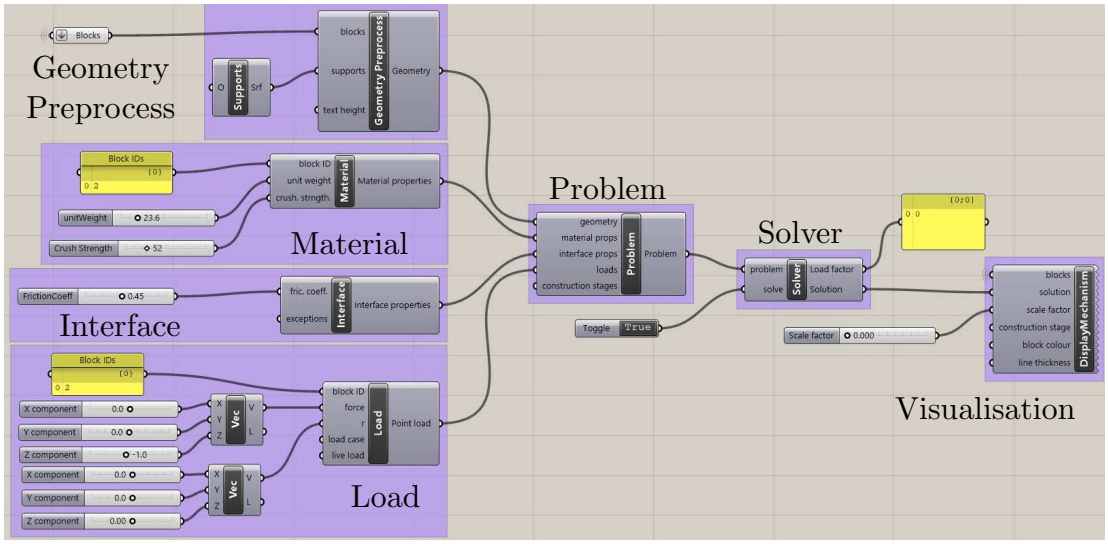

Figure 4: Computational design workflow for unreinforced stone masonry structures, illustrating the modular structure implemented within the Grasshopper environment, encompassing geometry preprocessing, material and interface properties, loading conditions, problem definition, solver, and collapse mechanism visualization.

The structural workflow begins with geometry, where the assembly is transferred to the *Geometry Preprocess* component as a collection of meshes, with each mesh representing a discrete block. This component also defines the support surfaces and au-

Table 1: Components of the Structural Analysis Workflow

No.	Component	Function
1	Geometry Preprocess	Identifies and generates interfaces between adjacent bricks and locates fixed boundary faces.
2	Material	Defines the unit weight and material strength of the blocks.
3	Interface	Assigns friction coefficients to the interfaces between blocks.
4	Load	Applies external forces and specifies their locations on the structure.
5	Problem	Integrates data from all preceding components and formats it for the RING solver.
6	Solver	Executes the RING limit analysis solver to compute the structural failure load.
7	Display Mechanism	Visualizes the computed failure mechanism (deformation) with a scale factor.

tomatically identifies the interfaces between adjacent blocks. The processed geometry is then passed to the *Problem* component, which acts as a central integrator. It combines the geometric data with material properties, interface characteristics, and loading conditions, which are assigned to the corresponding blocks. Subsequently, the *Solver* component uses an Application Programming Interface (API) to submit the complete problem definition to the LimitState:RING solver. The solver returns key results: the collapse load factor and the virtual displacement of each block at collapse. Finally, this displacement data is visualized within the Rhino environment, providing a graphical representation of the failure mechanism alongside the computed collapse load, as shown in Figure 5. Once the stability is verified, the resultant arch's geometric data are exported directly for generating a custom-fit cassette support structure.

2.3. Design for off-site construction

The core of the off-site construction technology presented here is a reusable cassette system developed for lifting and positioning unreinforced stone arches (see Figure 7a). The lightweight cassette design is crucial for minimizing material usage, reducing transportation costs, and facilitating efficient on-site assembly. Truss layout optimization

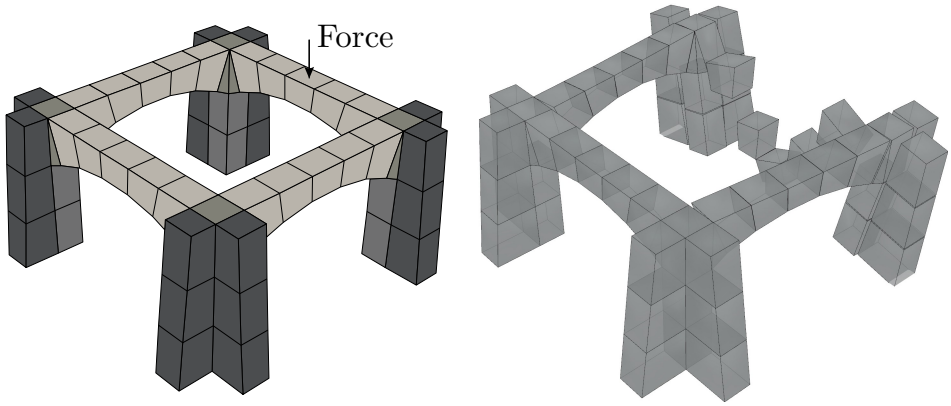

Figure 5: Visualization of a simple masonry structure with four bays under the single load imposed in the middle of an arch: (a) the parametric model (components differentiated by colour), and (b) the corresponding failure mode shown in Rhino.

[45, 46] is first applied to its frame design to generate a high-performance and minimum-volume cassette capable of supporting a pre-assembled stone arch. The standard layout optimization process, illustrated in Figure 6, begins with defining the design domain and boundary conditions (Figure 6a). Next, the design domain is discretized using nodes (Figure 6b), which are then interconnected with potential members to form a "ground structure" (Figure 6c). Finally, the optimum layout (Figure 6d) is identified by solving the following optimization problem,

$$\begin{aligned} \underset{\mathbf{a},\mathbf{q}^{(k)}}{\text{minimize}} \quad & V = \mathbf{l}^{\mathrm{T}}\mathbf{a} \\ \text{subject to} \quad & \mathbf{B}\mathbf{q}^{(k)} = \mathbf{f}^{(k)} \\ & -\sigma^{-}\mathbf{a} \leq \mathbf{q}^{(k)} \leq \sigma^{+}\mathbf{a} \\ & \mathbf{a} \geq \mathbf{0}, \end{aligned} \tag{1}$$

where V represents the total volume of members, $\mathbf{l}$ is a vector containing the lengths of each element $[l_1, l_2, \ldots, l_m]^{\mathrm{T}}$, the vector $\mathbf{a} = [a_1, a_2, \ldots, a_m]^{\mathrm{T}}$ signifies the cross-sectional areas of each element, $\mathbf{B}$ is a matrix of direction cosines, $\mathbf{q}^{(k)}$ denotes the axial force vector in each element for load-case k, and the vector $f^{(k)}$ represents the externally applied forces. σ^{+} and σ^{-} are the permitted stresses in tension and compression, respectively.

Subsequent to the truss layout optimization, geometry optimization is performed to relocate joint positions to more favorable configurations, aiming for a reduced structural volume (Figure 6e). This procedure may entail an automatic conversion of the structural model from a pin-jointed to a frame representation, thereby incorporating moment resistance at the joints. Finally, for the sake of reducing structural complexity, structural simplification is performed on the geometry optimization output to minimize the number of members, refer to Figure 6f. The background theory and algorithm are detailed in the reference [47].

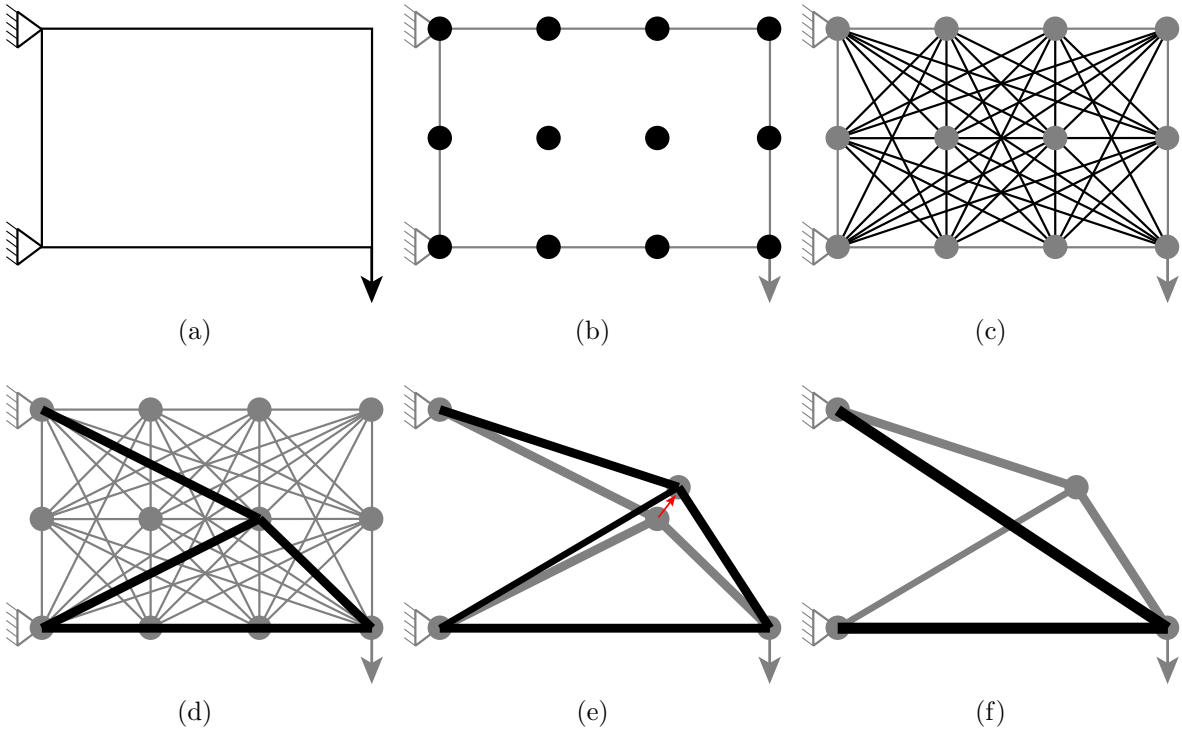

Figure 6: The standard truss layout optimization process: (a) define design domain and boundary conditions; (b) discretize domain using nodes; (c) interconnect nodes with potential truss members to form a 'ground structure'; (d) use optimization to identify the optimum layout; Post-processing steps: (e) geometry optimization; (f) structural simplification.

The optimal design for the supporting frame is derived from a parametric model of a simple, five-block arch, as illustrated in Figure 7a. The design domain, discretized with a nodal density of 10 and highlighted in dark grey, defines the region beneath the arch allocated for the frame. The optimization problem is formulated to minimize

the support frame's volume while maintaining adequate structural strength to bear the weight of the stone arch and resist bending moments. The process accounts for multiple loading conditions ($k = 5$), corresponding to the sequential placement of stone blocks (e.g., Blocks 1, 1+2, 1+2+3, 1+2+3+4, and 1+2+3+4+5), which represent the most critical phases of construction (see Figure 7b). To solve this problem, we employed Peregrine [48], a structural layout optimization plug-in for Grasshopper, which identifies the most efficient set of members from a dense initial ground-structure while satisfying the defined stress and equilibrium constraints.

The resulting optimized topology, obtained in a matter of seconds under the given nodal density, is shown in Figure 7c. It exhibits a distinct branching structure that effectively channels loads from the arch to the supports while minimizing material usage. This raw optimized design subsequently underwent geometry optimization and structural simplification to enhance fabricability, resulting in the practical cassette frame. A linear elastic analysis confirms that the maximum displacement under load is negligible relative to the frame's characteristic dimensions, validating its structural stiffness. Furthermore, while the optimization was based on one specific block placement sequence, a separate analysis verifies that the final design possesses the robustness to adequately support all other plausible construction sequences.

3. Application

To validate the feasibility and effectiveness of the proposed off-site construction method, a scaled physical model of a single arch was constructed and tested in a controlled laboratory environment. Due to safety restrictions and spatial constraints, the dimensions of a full-scale building were scaled down for laboratory testing, see Figure 8. This scaled model provided valuable insights into the practical application of the off-site construction method for unreinforced stone masonry structures. A parametric modelling approach confirmed the structural stability of the single arch model, where

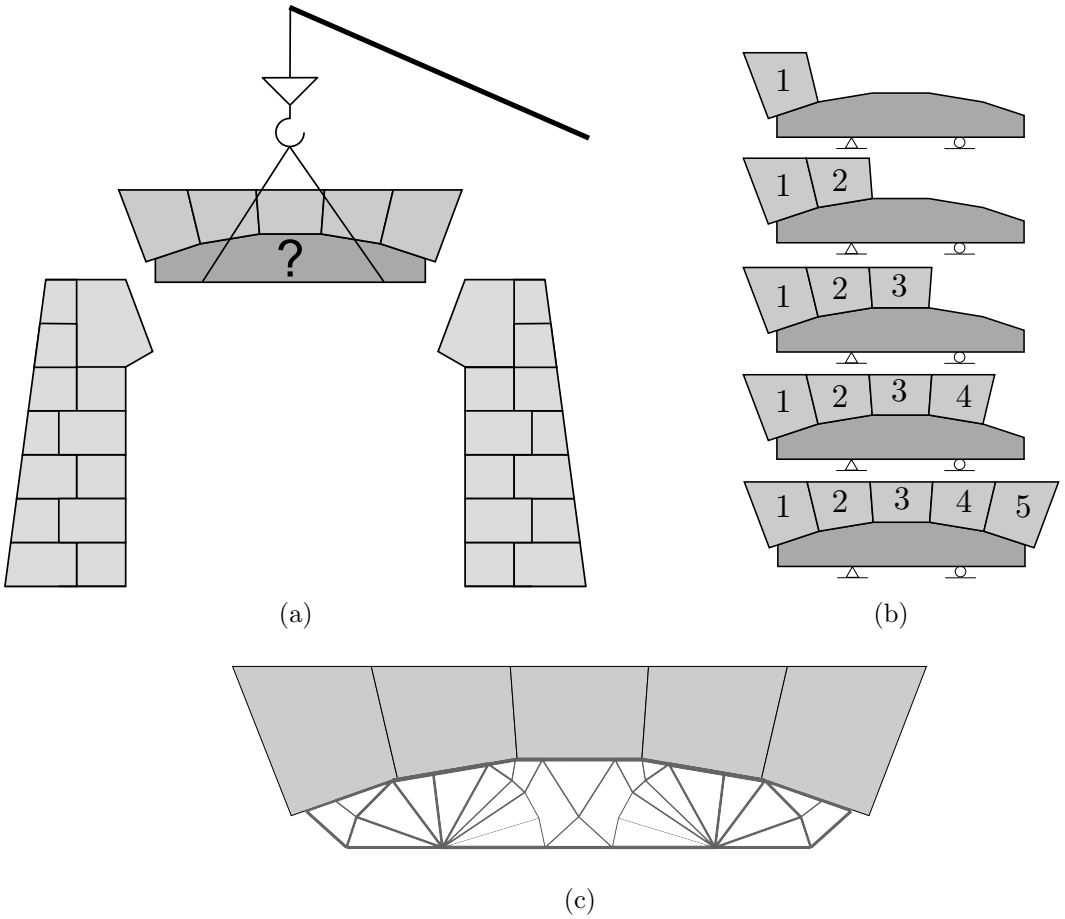

Figure 7: Overview of the design for the off-site construction: (a) the off-site technologies for unreinforced masonry construction focusing on the design of a cassette for lifting and positioning a stone arch, and the arch model (2D) consisting of 5 blocks showing the design domain (dark grey) for cassette optimization, (b) the multiple loading conditions that arise during the sequential placement of the stone blocks, and (c) optimized frame topology for supporting the pre-assembled arch.

the analysis employed block material properties of 2400 kg/m^3 for density, 50 MPa for compressive strength, and an interface friction coefficient of 0.8.

3.1. Blocks

While the original concept focuses on pre-fabricated stone components, concrete blocks were used in this experiment. This material substitution maintained the fundamental principles of the off-site construction methodology, allowing for a proof-of-concept demonstration of the assembly process and structural performance. To simplify the concrete casting process, certain geometric modifications were implemented. Notably, the buttress shape was simplified from a trapezoidal to a rectangular configu-

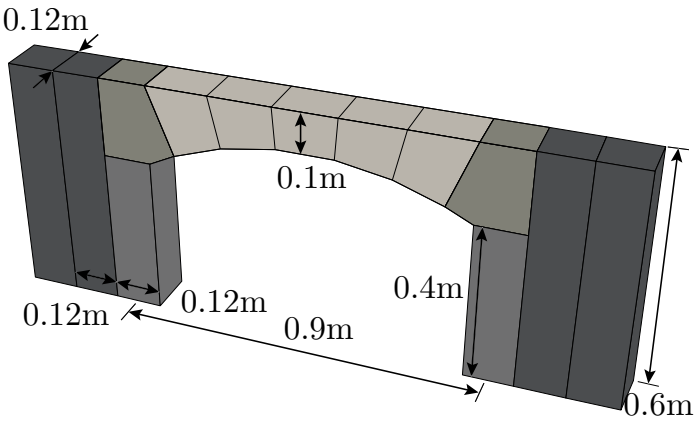

Figure 8: A scaled single arch model with the geometric configuration used in the experimental validation, comprising an arch with five blocks, two springer blocks, two column blocks, and four buttress blocks.

ration. As the columns and buttresses are not the main focus of this project, this does not significantly affect the conclusions. The final model comprises four concrete blocks for the buttresses, two blocks for the columns, two springer blocks to transition between the vertical columns and the arch, and five blocks forming the arch itself. For the non-rectangular blocks in the arch and springers, Polylactic Acid (PLA) 3D printing was used to create moulds of the required shapes. Figure 9 provides a visual representation of the actual concrete arch blocks fabricated for the experiment. To accommodate the adjustable boxes with vertical bars within the cassette (discussed in the following section), which provide essential horizontal support to the arch blocks, strategically positioned holes are drilled into the base of the arch blocks. This allowed the vertical dowels to pass into the blocks, securing them within the cassette and ensuring stability during lifting and placement.

Figure 9: Concrete arch blocks casted for the off-site construction test.

To determine the physical properties of the concrete blocks, their densities were measured. The average value was found to be $2360\,\mathrm{kg/m^3}$, consistent with the expected density of typical concrete mixes. Next, we identified the friction coefficient at the interface between the arch blocks and springer blocks. A tilting table apparatus equipped with a level box was employed to induce movement in the blocks and accurately measure the corresponding tilting angle at the onset of motion, see Figure 10. This method allowed for direct assessment of the static friction coefficient. The experimentally determined friction coefficient, ranging from 0.40 to 0.55, significantly deviated from the idealized 0.8 used in our numerical model. This discrepancy arose from variations in surface texture and flatness among the concrete blocks, a consequence of the inherent inconsistencies in concrete casting. As these concrete blocks are designed to model natural stone, variability will also exist in real-world use of this technique. The prevalence of sequential failure modes in masonry arches, characterized by initial sliding followed by hinge formation under high-strain conditions, underscores the critical importance of frictional properties. Consequently, accurately quantifying the friction coefficient is not merely supplementary but fundamental to any structural analysis aiming to reliably predict the full load-bearing capacity of the structure.

3.2. Cassette

The optimized frame (see Figure 7c), obtained by considering the arch block loading sequence, forms the skeleton of the final cassette design. While the cassette frame provides effective vertical support for the stone arch, ensuring stability in the horizontal and out-of-plane directions requires further consideration. To achieve complete arch support, the optimized frame design is enhanced with several key features, illustrated in Figure 11 and described below:

- The final cassette frame design incorporates the key features of the numerically optimized design, and several modifications are necessary to ensure practical feasibility and structural integrity, see Figure 12. These modifications include: an

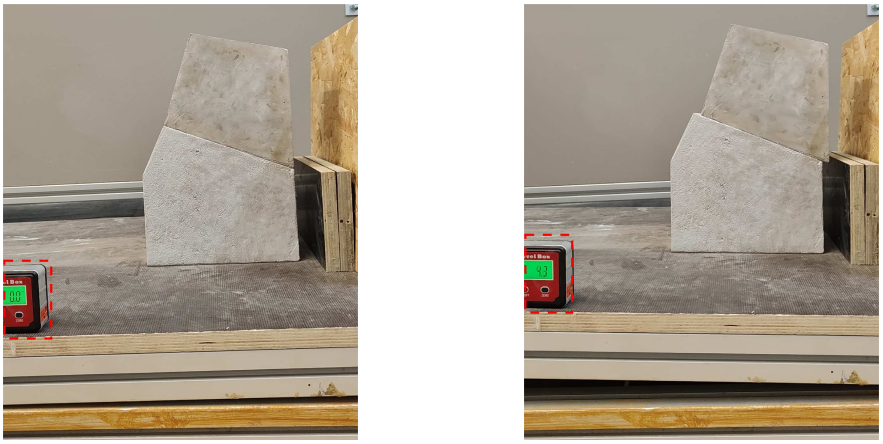

(a) (b)

Figure 10: Friction test setup for a block interface: (a) initial state of blocks on a tilting table. The table's inclination is gradually increased while a digital level (bottom left) indicates the angle relative to the horizontal. Note that the block interface is not parallel to the table surface and the bottom block does not move; (b) sliding initiated at the critical angle. The critical angle is reached when the block begins to slide. The final friction angle of the block interface is determined by adding the angle shown in the level box to the angle between the block interface and the tilting table surface.

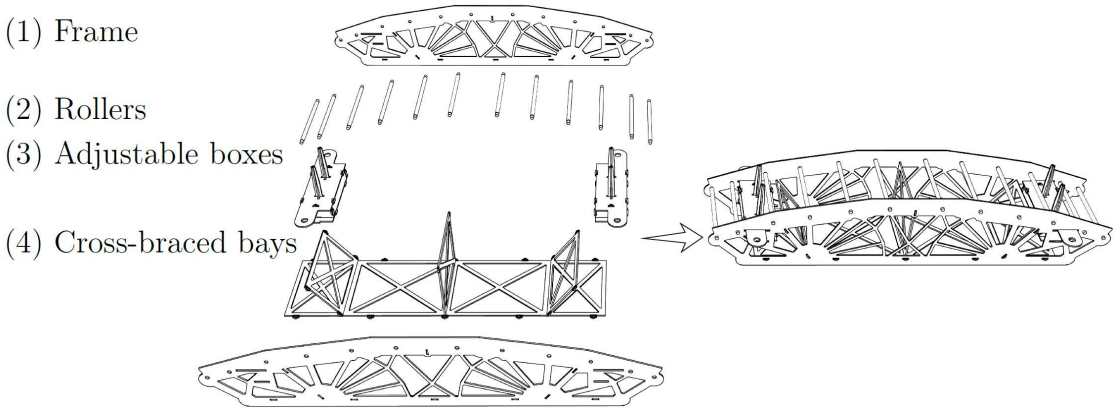

Figure 11: Final cassette design featuring key components for secure placement of the pre-assembled stone arch: (1) optimized frames with 'skirting' for out-of-plane constraint, (2) rollers connecting the cassette frames to the vertical support, (3) adjustable boxes with vertical bars for horizontal support, and (4) cross-braced bays for overall stability.

adjusted layout in region ① to accommodate the box for horizontal support, reinforcement in region ② to mitigate the risk of local failure, and the addition of 'skirting' (region ③) along the top edge to constrain out-of-plane movement of the stone arch and maintain the structural integrity during lifting and positioning.

- Rollers are integrated into the top edge of the cassette, connecting the individual

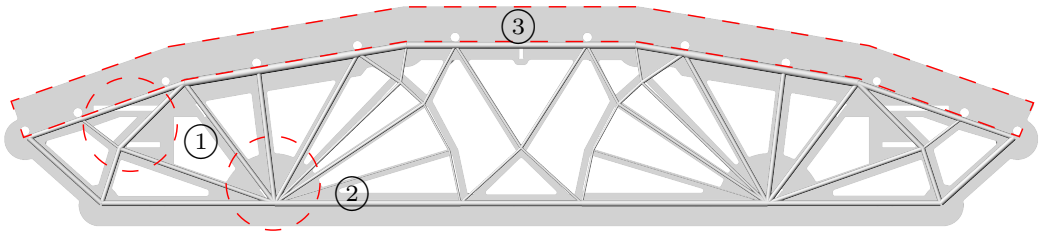

Figure 12: The final cassette frame design (background) is shown in relation to the initial numerically optimized design. Key adaptations include: a modified layout in region ① to accommodate the horizontal support box, reinforced material in region ② to prevent local failure, and the addition of 'skirting' (region ③) at the top to constrain block movement perpendicular to the frame.

optimized frames. These rollers serve a dual purpose: they stiffen the cassette and distribute the arch's weight evenly across the frame, mitigating potential stress concentrations; and, critically, they facilitate cassette reusability for arches of identical span and width but varying rise (curvature), achieved by employing rollers of differing diameters.

- Horizontally, sliding adjustable boxes are connected to the cassette frame moving on slotted guide rails, see Figure 13, featuring strategically positioned vertical dowels that pass through the stone blocks. These dowels provide crucial lateral restraint, counteracting horizontal thrust forces and ensuring the arch remains securely positioned within the cassette during placement. The adjustability of these dowels allows for fine-tuning during assembly, accommodating minor variations in the stone block dimensions and ensuring a precise fit within the arch. To minimize imperfections and ensure flush contact between arch blocks, the horizontal boxes are connected using turnbuckles/ratchet straps. This system binds the blocks together, mitigating potential defects and uneven interfaces arising from the fabrication and cutting processes.

- To further enhance the structural integrity of the cassette, cross-braced bays are incorporated throughout the frame. This reinforcement increases the overall stiffness and load-bearing capacity of the cassette, minimizing deflection and ensuring

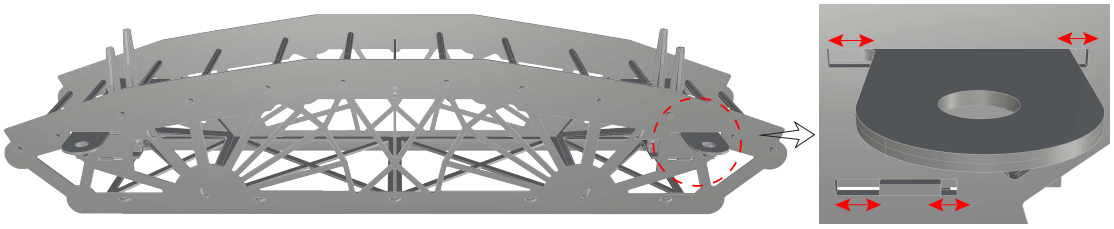

Figure 13: Detail of the adjustable support mechanism integrated with the cassette frame. The highlighted components (red dashed circle) are horizontally adjustable boxes equipped with vertical bars, which ensure lateral stability of the stone arch. This adjustability is crucial for precise alignment and for accommodating variations in as-built block geometry.

the safe erection of the arch. The bracing also spaces the main arch planes at precisely the correct separation distance.

This integrated system, comprising optimized frames, rollers, adjustable boxes with vertical bars, and cross-braced bays, provides a comprehensive solution for the stable and accurate positioning of the pre-assembled stone arch throughout transportation and on-site placement.

The cassette was fabricated in partnership with Unipart Construction Technologies using advanced manufacturing techniques, specifically laser cutting of steel sheet with special mechanical fasteners. All components, with the exception of the top rollers, were laser-cut from 2 mm steel plate, see Figure 14. Excess material was easily removed, followed by edge deburring and polishing to achieve a smooth edge and surface finish. Interlocking slot rivet features were incorporated into the design to securely join pieces together, eliminating the need for welding (which can cause distortion of the steel during fabrication) during cassette assembly. Two laser-cut frames were connected by cross-braced bays and rollers. Adjustable boxes were made with rails running on slots laser cut into the main side plates, the boxes included vertical dowels to catch the horizontal thrusts from the end blocks which were then attached to the frames, with designed clearances to permit horizontal movement of the boxes. Finally, socket head cap screws, steel round tubes, and heat shrink wraps were integrated with the top rollers.

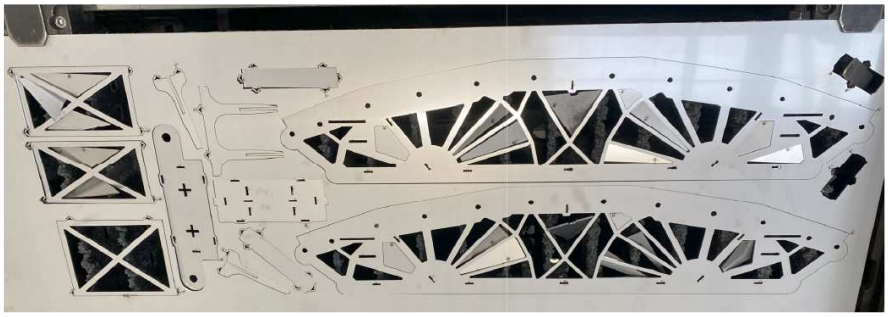

(a) Laser-cut steel plate

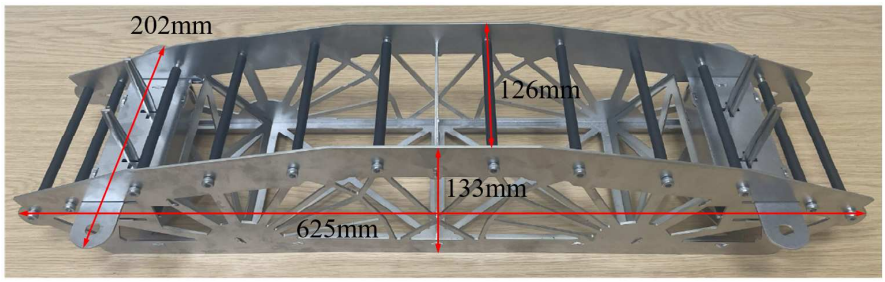

(b) Final cassette

Figure 14: Fabrication and assembly of the reusable cassette: (a) Laser cutting of 2 mm steel plate to produce the structural components; (b) The fully assembled cassette, with critical dimensions labeled. The cassette has a maximum length of 625 mm, a maximum width 202 mm, a maximum height 133 mm, and an internal frame spacing of 126 mm.

3.3. Lifting apparatus

Due to the reduced size of the laboratory scale test sample, it was not possible to directly connect the lifting chains to the lifting points on the cassette (see Figure 19 below). Therefore, to facilitate the lifting of the pre-assembled arch by crane, a specialized lifting apparatus was designed and fabricated. The setup used for the reduced scale tests reported here is shown in Figure 15, and consists of four main components:

- Base plate: This robust plate serves as the foundation of the apparatus, providing a secure platform for supporting both the cassette and the pre-assembled arch.
- Clamps: To prevent any unintended movement or shifting during lifting, extra clamps were strategically employed to firmly secure the cassette to the base plate.
- Threaded bars: Four high-strength adjustable vertical bolts rigidly connected the top and base steel plates, ensuring effective transfer of lifting forces and overall

system stability.

- Top plate with hoist rings: A sturdy top plate, equipped with two hoist rings, was connected to the base plate via four vertical bolts. These hoist rings provided secure attachment points for the crane's lifting hooks, ensuring a balanced and stable lift.

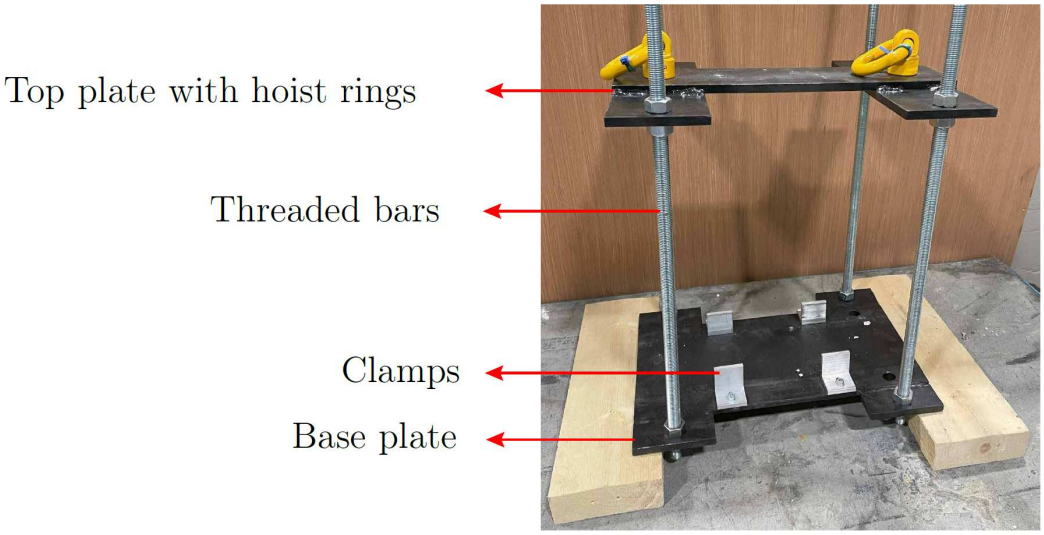

Figure 15: Configuration of the custom lifting apparatus designed for the safe handling of the pre-assembled stone arch. The apparatus consists of a base plate (400 mm × 300 mm) with four integral clamps to secure the cassette. Structural rigidity is achieved through four vertical, adjustable threaded bars (800 mm long), which connect the base to an identical top plate equipped with hoist rings for crane lifting.

3.4. Demonstration

Prior to assembly, specific masonry components, including columns, buttresses, and springer blocks, were positioned and secured. While transportation was not a primary concern for this laboratory investigation, the cassette's integrated skirting and adjustable boxes provide effective constraint against block movement during transport, if required. The experimental procedure comprised two phases: (1) off-site pre-assembly of the arch within the cassette (Figure 16), and (2) on-site installation of the assembled arch into the masonry structure (Figure 17). The following procedure was employed:

1a Positioning and securing the cassette: The base plate of the lifting apparatus was positioned on top of the timber boards, ensuring a stable and level foundation. The cassette was placed onto the base plate and firmly secured using several clamps. This prevented any lateral movement or shifting of the cassette during the subsequent lifting process.

1b Placing the arch blocks: The arch blocks were positioned on top of the cassette. The adjustable horizontal boxes with vertical dowels provided adequate horizontal support to the arch and ensured lateral stability during lifting. These boxes were carefully adjusted to ensure a snug fit and prevented any undesirable movement of the arch blocks. Turnbuckles/ratchet straps were attached and tightened to close the inter-block gaps.

1c Assembling the lifting apparatus: The top plate of the lifting apparatus was then secured to the base plate by inserting and tightening the vertical bolts. This completed the assembly of the lifting apparatus allowed for the secure attachment of the arch and cassette to the crane, ensuring a safe and controlled lift.

2a Lifting and positioning: The integrated system, comprising the arch, cassette, and lifting apparatus, was then attached to a crane using the hoist rings on the top plate. Careful attention was paid to ensure a balanced and secure connection to the crane's lifting hooks. The crane carefully lifted the entire assembly and positioned it at the desired location.

2b Resetting the cassette: Once the arch was in place, the cassette was removed from beneath the arch and placed onto a trolley. The top plate and vertical bolts of the lifting apparatus were detached and lifted, and the cassette was returned to its original location to prepare for the next arch assembly.

This systematic approach ensured the safe and controlled lifting and placement of the pre-assembled arch, minimizing the risk, time and manual input required for the on-site phases. By focusing on the lifting process, we were able to efficiently assemble and

position the arch within the laboratory setting.

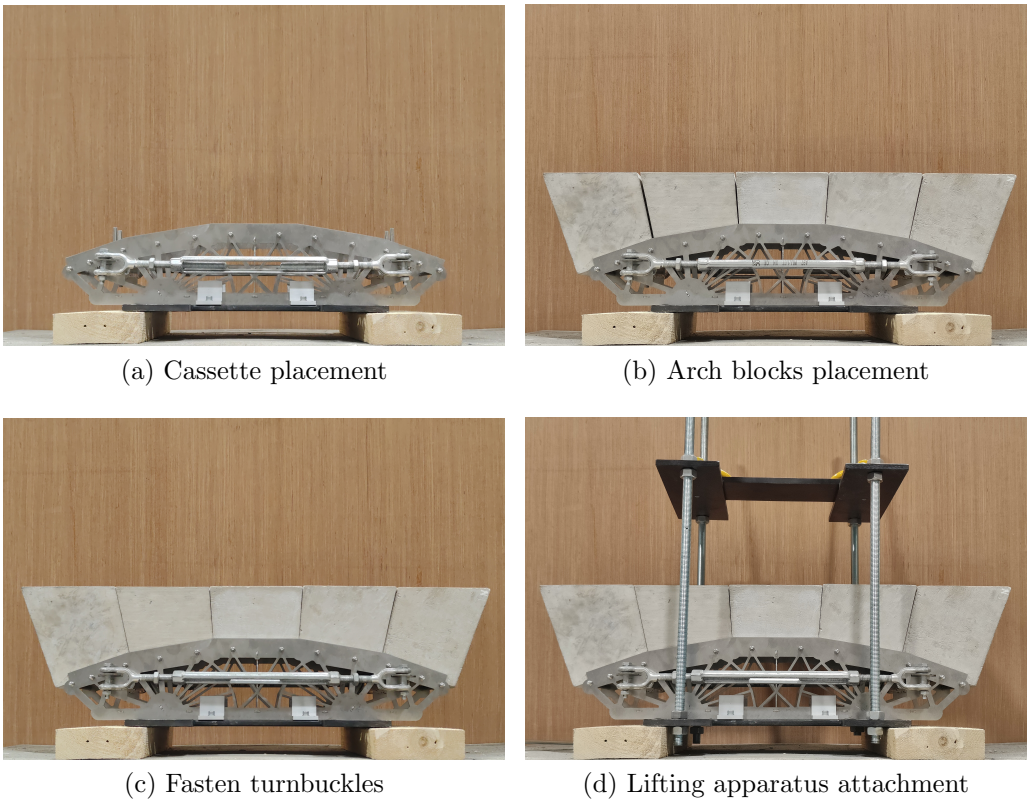

(a) Cassette placement (b) Arch blocks placement

(c) Fasten turnbuckles (d) Lifting apparatus attachment

Figure 16: Off-site pre-assembly procedure for the integrated arch blocks and cassette. The sequence is as follows: (a) The cassette with turnbuckles is positioned and firmly anchored to the base plate of the lifting apparatus. (b) Each block is then carefully placed, with its position stabilized by the adjustable support boxes. (c) The turnbuckles are progressively tightened to eliminate tolerances and achieve full compression across all voussoir joints. (d) The structural rigidity of the system is ensured by installing the threaded bars and attaching the top lifting plate with its hoist rings.

4. Results and Discussion

The investigation provided valuable insights into the performance of the off-site pre-fabricated arch and its interaction with the supporting structure, validating the proposed construction method. By replicating key on-site assembly stages within a controlled laboratory environment, the structural behavior of the arch during the critical lifting and placement phase was closely monitored and analyzed. The resulting masonry structure exhibited structural integrity and stability, highlighting the potential of off-site construction to enhance the efficiency and safety of unreinforced masonry

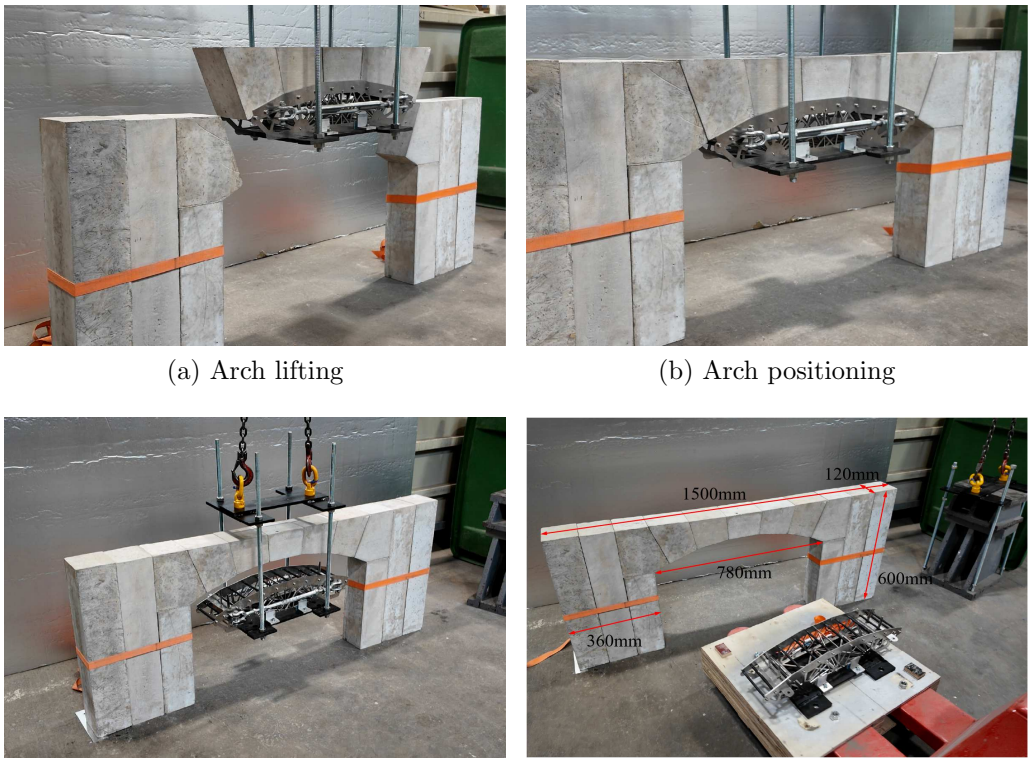

(a) Arch lifting (b) Arch positioning

(c) Cassette removal (d) Lifting apparatus disassembly

Figure 17: Key stages of the on-site construction process: (a) Crane-assisted lifting of the pre-assembled arch; (b) Guided lowering and careful alignment of the system into its final position; (c) Structural decoupling, achieved by extracting the vertical bars from the adjustable boxes to release the arch; (d) Breakdown and recovery, showing the lifting apparatus being moved via trolley for disassembly and the readying of the cassette for subsequent use.

construction. The entire process, from integrating the arch blocks with the cassette to the final disassembly of the lifting apparatus, was completed in approximately 15 minutes. This total duration was evenly split between off-site pre-assembly and on-site operations. A review of the process timelines revealed that the most time-consuming tasks across both phases were those associated with the assembly and disassembly of the lifting apparatus itself. The following sections detail specific findings regarding the cassette system's performance, the accuracy of the assembly process, and the structural behavior of the constructed arch.

4.1. Off-site construction validation

The optimized, frame-based cassette design demonstrated satisfactory performance during testing, successfully meeting all pre-defined design requirements. No plastic deformation of the cassette structure was observed, indicating its structural integrity under the applied loads. The incorporated 'skirt' and adjustable boxes proved effective in positively constraining the individual arch blocks, ensuring a precise and consistent fit within the cassette, a result attributed to the carefully considered fabrication tolerances and laser cut precision. During the assembly of the blocks onto the cassette, several placement sequences are possible, one such sequence is shown in Figure 18. Initial inter-block gaps measured prior to the application of turnbuckle tension were in the range of 1 to 8 mm. A clear trend was observed where gap magnitudes increased towards the side blocks, a consequence of the arch's inherent horizontal thrust before it is fully constrained. While manual handling was feasible for the scaled model due to the low block weight, further design development of the cassette and arch block placement mechanisms will be required for a full-scale application.

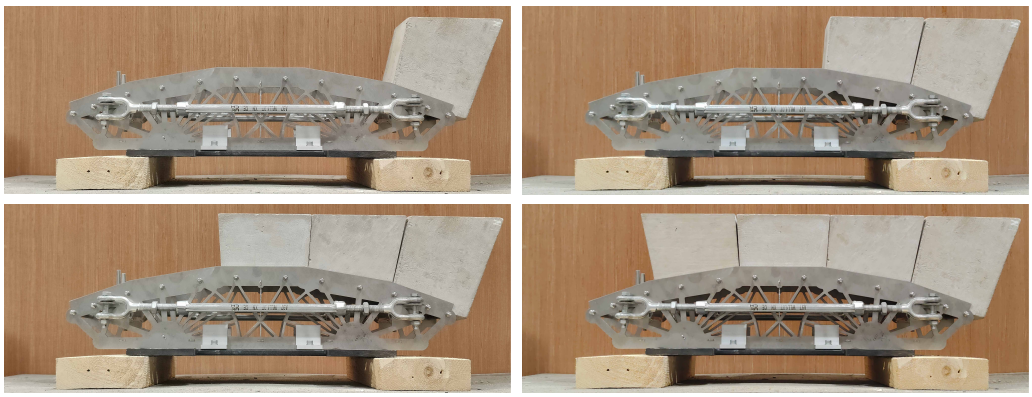

Figure 18: A representative construction sequence demonstrating the placement of arch blocks from right to left. The structural stability observed at all intermediate stages validates the design of the support cassette, which is required to carry partial and asymmetric loads during assembly.

While the successful integration of the lifting apparatus demonstrated the potential of the cassette system for efficient and accurate off-site construction of masonry arch structures, further investigation is required for larger-scale testing under more rigorous

loading conditions. For practical applications, a refined integrated lifting system is recommended. The current apparatus, while functional, exhibits certain redundancies (e.g., the base and top plates) and limitations in practicality. Figure 19 presents a conceptual design for a revised system, incorporating chains instead of threaded bars for direct cassette attachment (eliminating the base plate), and a spreader frame (replacing the top plate) to connect the chains. As the chain connects to an overhang integrated into the cassette design, it is crucial to consider this connection point during the optimization process to ensure sufficient material is allocated to resist the induced bending moment.

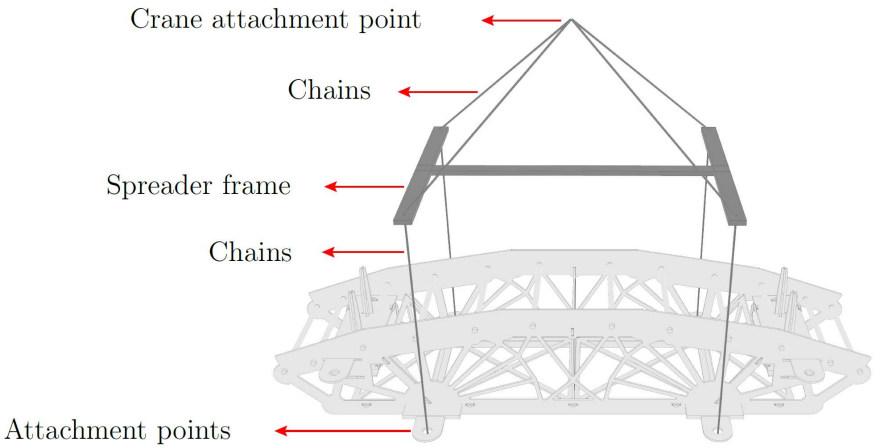

Figure 19: Conceptual design for an evolved lifting system, proposing the use of chains and a spreader frame to directly engage with the cassette. This configuration is intended to offer greater flexibility and faster setup compared to the rigid threaded bar system.

Two methods for securing the adjustable boxes, turnbuckles and ratchet straps, were evaluated during testing to provide horizontal support to the arch blocks. Both methods demonstrated effective performance in minimizing the inter-block gaps within this scaled model, as illustrated in Figure 20. While both successfully reduced the gaps, the turnbuckles offered finer-grained control over the adjustment, allowing for more precise manipulation of the arch block positioning. The ratchet straps, while providing secure clamping force, offered a quicker and potentially more efficient means of securing the boxes. The choice between turnbuckles, ratchet straps and their combinations would

likely depend on the specific requirements of the full-scale application, considering factors such as the desired level of precision, the speed of assembly, and the overall cost. Further investigation into the long-term performance and durability of each method under repeated loading and environmental conditions would be beneficial for a comprehensive comparison. It is expected that availability of such components will be highly dependent on scale, so further studies are recommended to be undertaken alongside larger scale tests.

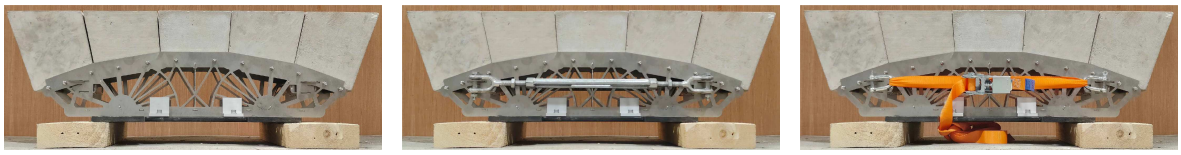

(a) The inter-block gap (b) Turnbuckle (c) Ratchet strap

Figure 20: Application of tensile force to the adjustable support boxes to eliminate (a) inter-block gaps and ensure full contact between voussoirs. The two implemented tensioning systems are (b) a finely-adjustable turnbuckle and (c) a high-capacity ratchet strap.

Precise placement of the pre-assembled arch, illustrated in Figure 21, required careful intervention during both lifting and positioning. Crane operation was critical for hoisting the integrated system, during which a maximum transient lateral deflection of approximately 15 mm was observed. This deflection, a dynamic response to crane motion, remained within acceptable limits. Once roughly in place, minor adjustments were necessary to achieve accurate final positioning. To facilitate this process, the incorporation of guide elements is suggested for future studies. These guides could be integrated either onto the springer blocks, providing a 'catch' for the pre-assembled arch during placement, or within the cassette itself, aiding in the accurate positioning of the arch during assembly and subsequent lifting. Either approach would likely improve the efficiency and precision of the arch placement process.

The cassette reset procedure, particularly the safe removal of the cassette from beneath the positioned arch, required careful consideration to prevent damage. Releasing the fastening equipment was essential to minimize friction between the vertical bars

(a) (b)

Figure 21: Manual interventions for precise arch placement: (a) Guided stabilization during crane-assisted lifting to control swing and orientation; (b) Fine-adjustment of the arch's position using controlled, light tapping to achieve final alignment.

of the adjustable box and the arch blocks. A trolley, positioned beneath the arch, facilitated the placement and subsequent disassembly of the lifting apparatus. While successful in the controlled laboratory environment, this procedure may pose challenges in full-scale applications, especially where under-arch access is limited. Some of these issues will be alleviated by the typical detailing that would be expected at full scale (e.g. lifting hooks) compared with those used for the small scale test here (i.e. threaded bar and bolts). Future research should investigate alternative lifting apparatus removal strategies, including methods for dismantling the apparatus from above the completed masonry structure.

4.2. Masonry structural performance

The assembled masonry structure resulting from the proposed off-site construction methodology is depicted in Figure 22. While the focus of this project was the arch assembly, the columns, buttresses, and springer blocks were positioned prior to arch placement. For simplification of concrete casting, the buttresses and columns were designed as three separate rectangular blocks. Although our numerical model indicates overall structural stability, the imperfect connection between the column and buttress components could potentially limit the structure's load-bearing capacity, particularly in supporting the arch. To address this and ensure adequate lateral support, ratchet

straps were employed to effectively unify the three separate blocks, enabling them to function as a single, cohesive unit.

(a) Front view (b) Rear right view

Figure 22: Completed masonry structure assembled using the proposed off-site construction technique: (a) front view and (b) rear right view.

During the arch placement process, small movements of the buttresses were observed upon contact between the pre-assembled arch and the springer blocks. This movement is attributed to a combination of factors, including the horizontal thrust exerted by the arch, initial slack in the ratchet straps securing the buttresses, imperfect contact at the column-buttress and buttress-buttress interfaces, and potential initial misalignment of the buttresses themselves. Despite this, the pre-assembled arch remained stable throughout the lifting and positioning phases. Figure 23a details the interface between the springer and arch blocks, revealing a seemingly limited contact area, primarily along the bottom edge. This may be due to non-flat block interfaces and minor inaccuracies in the positioning of the springer blocks and columns. This limited contact area warrants further investigation to assess its long-term structural implications. However, it should be noted that this test was carried out without mortar, which would contribute to filling gaps such as these.

The use of a dry-joint system in this prototype prioritizes rapid, precise, and automated assembly, aligning with off-site prefabrication principles. The cassette system ensures stability through geometric interlock and compression by achieving tight tolerances that minimize gaps. While effective for proof-of-concept, the absence of mortar presents limitations for permanent structures, notably a reduced capacity to accom-

modate geometric imperfections, mitigate point stresses, and provide weather-proofing. Incorporating mortar would enhance durability, load distribution, and robustness but introduces complications such as curing time, mess, and reduced construction reversibility. Therefore, future research will explore the integration of mortar into this workflow, developing techniques for its application within the cassette system to create a hybrid process that balances assembly efficiency with the enhanced performance of a mortared masonry structure.

(a) Gap between springer and arch blocks (b) Damage and misalignment

Figure 23: Issues identified during practical test: (a) Limited contact area between springer and arch blocks, primarily along the bottom edge; (b) Damage near the vertical dowel holes in the arch blocks, likely caused by dowel insertion/removal, and minor misalignment of blocks.

Following some iterations of assembly and disassembly, minor damage was observed near the holes in the arch blocks (Figure 23b), likely resulting from the insertion and removal of the vertical dowels during the assembly/disassembly process. This suggests the need for design refinements to protect these critical areas during handling. Additionally, slight misalignment between the arch blocks was detected after final positioning. This misalignment is likely attributable to a combination of factors, including tolerances in the cassette fabrication and potential discrepancies between the drilled hole locations and the vertical dowel positions. Further analysis of these tolerances and drilling procedures is recommended to minimize future misalignments and improve the overall precision of the off-site construction process. The observed buttress movement, limited springer block contact, damage near the vertical bar holes, and minor misalign-

ment highlight areas for potential improvement in the proposed off-site construction methodology.

4.3. Implications for modern unreinforced masonry construction

The conducted tests demonstrate that the proposed off-site construction method offers several advantages over traditional stone arch construction. By reducing reliance on specialized on-site masonry skills, this approach can increase the accessibility and affordability of stone masonry, promoting its wider adoption. However, several limitations require further investigation. First, a comprehensive life-cycle assessment, encompassing all materials including the steel used in cassette fabrication, is necessary to fully quantify the environmental benefits of stone masonry structures. Second, practical challenges associated with full-scale implementation, such as safe and efficient placement of heavy stone blocks at significant heights, require further research and development. Finally, the current design, requiring separate lifting apparatus and trolley for cassette manipulation, could be optimized by integrating these components into a single, streamlined system for improved efficiency and reduced on-site complexity. To further enhance this off-site construction method for modern stone masonry structures, several key areas have been identified for future development.

- Enhanced parametric modelling: The current computational model used for design and analysis can be further refined by incorporating additional factors that influence the structural behaviour. Specifically, integrating the mechanical properties of the mortar and the impact of interface flatness between blocks will improve the accuracy and predictive capabilities of the model. This will enable more realistic simulations of the arch's response to loading and environmental conditions.

- Adaptive cassette design: The current cassette design, while functional, could be optimized to accommodate a wider range of arch geometries and configurations.

For instance, implementing adjustable components within the cassette will allow for variations in arch span, width, and block dimensions. This adaptability will significantly increase the versatility of the system and its applicability to diverse architectural designs. Furthermore, a modular design approach, where the cassette is comprised of smaller, interchangeable units, will enhance its reusability and adaptability. This will allow for the assembly of cassettes tailored to specific arch geometries, minimizing material waste and improving construction efficiency.

- Broader applications: The cassette-based assembly method can be adapted for the construction of complex vaulted ceilings and domes, enabling the prefabrication of these intricate structures in a controlled environment. Moreover, this method has significant potential for the restoration and conservation of historical masonry structures. The ability to prefabricate arches and other structural elements off-site minimizes on-site disruption and allows for precise replication of original architectural details.

5. Summary and conclusion

This paper introduces a novel approach to modernize unreinforced stone masonry construction, integrating off-site fabrication with advanced computational design. Driven by the environmental advantages of stone as a low-carbon building material, this research focuses on developing an efficient and precise assembly method for unreinforced masonry structures. The core of this method lies in the integration of parametric design, structural analysis, and an off-site construction strategy based on a specialized, optimized cassette system for placing pre-assembled stone arches. A truss layout optimization algorithm guided the design of this cassette, ensuring arch structural integrity during erection. The optimized cassette frame incorporates rollers, cross-braced bays, and adjustable vertical dowels for pre-assembling arches. A scaled physical model was fabricated and tested to validate the feasibility of the proposed reusable cassette sys-

tem. Experimental results confirm the effectiveness of the integrated cassette and lifting apparatus in achieving accurate and efficient assembly of the arch masonry structure.

The optimized, frame-based cassette design performed satisfactorily, effectively constraining blocks into a pre-assembled arch. Both turnbuckles and ratchet straps were effective in minimizing inter-block gaps, with turnbuckles providing more precise control over the alignment process. The current lifting apparatus fulfilled its intended function; however, conceptual designs for an enhanced, integrated lifting system hold significant potential for large-scale implementations. Furthermore, the study highlighted the critical role of precise crane operation and suggested guide elements to facilitate accurate arch placement. Regarding masonry structural performance, initial challenges with supporting structure connections were overcome by using ratchet straps to unify separate buttress blocks, enhancing lateral support. While minor buttress movements were observed during arch placement, the arch remained stable. Notably, the limited contact area at the springer-arch interface warrants further investigation, particularly as the tests were conducted without mortar. Additionally, minor damage near arch block dowel holes and slight inter-block misalignment after final positioning indicate a need for more stringent control over drilling procedures to enhance overall precision. Looking ahead, the development of an advanced, intelligent cassette design represents a key area of focus. Such a design should be capable of effectively constraining arch blocks while simultaneously preventing any potential damage, thereby optimizing both the construction process and the long-term performance of masonry structures. Overall, this research demonstrates the potential to enhance the efficiency, precision, and scalability of modern stone construction while promoting the use of stone as a sustainable building material.

The methodology established in this work provides a scalable and adaptable framework that extends beyond the single arch demonstrated here. The underlying principles of parametric design, structural optimization, and off-site pre-assembly are readily ap-

plicable to more complex masonry geometries, such as multi-arch sequences. Future research will focus on extending this workflow to these larger assemblies and exploring the integration of irregular or reclaimed stone units. Furthermore, the cassette-based system presents a viable platform for the future integration of on-site robotic assistance, which could automate positioning and locking sequences to achieve unprecedented levels of speed and precision. By advancing these directions, this approach can significantly broaden the application of stone masonry, facilitating its use in a wider range of sustainable and architecturally expressive structures.

Declaration of Competing Interest

The authors declare that they have no known competing financial interests or personal relationships that could have appeared to influence the work reported in this paper.

Acknowledgment

Professor Matthew Gilbert passed away before the submission of this manuscript. He contributed significantly to the conceptual development of the work, and his coauthorship is included with deep respect and gratitude.

The authors gratefully acknowledge financial support from the Engineering and Physical Sciences Research Council Impact Acceleration Account (grant no. S16213). The authors are particularly grateful to Kieran Nash, Samuel J Gibson, John Earnshaw, and Kieren Howarth for their expert technical assistance and dedicated support in the heavy structure lab and workshop.

Data availability

Data will be made available on request.

References

[1] Pere Roca, Paulo B Lourenço, and Angelo Gaetani. *Historic construction and conservation: materials, systems and damage*. Routledge, 2019.

[2] Siegfried Siegesmund, Tom Weiss, and Axel Vollbrecht. *Natural Stone, Weathering Phenomena, Conservation Strategies and Case Studies*. Geological Society of London, 01 2002.

[3] Firas Sharaf. The impact of thermal mass on building energy consumption: A case study in al mafraq city in jordan. *Cogent Engineering*, 7(1):1804092, 2020.

[4] K Ramamurthy and E K Kunhanandan Nambiar. Accelerated masonry construction review and future prospects. *Progress in Structural Engineering and Materials*, 6(1):1–9, 2004.

[5] Huu-Tai Thai, Tuan Ngo, and Brian Uy. A review on modular construction for high-rise buildings. *Structures*, 28:1265–1290, 2020.

[6] Lara Jaillon and C.S. Poon. Life cycle design and prefabrication in buildings: A review and case studies in hong kong. *Automation in Construction*, 39:195–202, 2014.

[7] Rui Jiang, Chao Mao, Lei Hou, Chengke Wu, and Jiajuan Tan. A swot analysis for promoting off-site construction under the backdrop of china's new urbanisation. *Journal of Cleaner Production*, 173:225–234, 2018. Sustainable urban transformations towards smarter, healthier cities: theories, agendas and pathways.

[8] Zhuo Cheng, Shengxian Tang, Hexu Liu, and Zhen Lei. Digital technologies in offsite and prefabricated construction: Theories and applications. *Buildings*, 13(1):163, 2023.

[9] Xialu Liu, Chao Hou, Jiahao Peng, Yuyin Wang, and Kim J.R. Rasmussen. Recent advancements of inter-module connections for modular buildings: An overview and multi-dimensional assessment. *Engineering Structures*, 335:120378, 2025.

[10] Charles M. Eastman and Rafael Sacks. Relative productivity in the aec industries in the united states for on-site and off-site activities. *Journal of Construction Engineering and Management*, 134(7):517–526, 2008.

[11] Xin Hu, Heap-Yih Chong, Xiangyu Wang, and Kerry London. Understanding stakeholders in off-site manufacturing: A literature review. *Journal of construction engineering and management*, 145(8):03119003, 2019.

[12] Paul M Goodrum, Dong Zhai, and Mohammed F Yasin. Relationship between changes in material technology and construction productivity. *Journal of construction engineering and management*, 135(4):278–287, 2009.

[13] Pablo Martinez, Michelle Livojevic, Purvish Jajal, Daniel Ryan Aldrich, Mohamed Al-Hussein, and Rafiq Ahmad. Simulation-driven design of wood framing support systems for off-site construction machinery. *Journal of Construction Engineering and Management*, 146(7):04020075, 2020.

[14] Jack Steven Goulding, Farzad Pour Rahimian, Mohammed Arif, and MD Sharp. New offsite production and business models in construction: priorities for the future research agenda. *Architectural engineering and design management*, 11(3):163–184, 2015.

[15] Ruoyu Jin, Shang Gao, Ali Cheshmehzangi, and Emmanuel Aboagye-Nimo. A holistic review of off-site construction literature published between 2008 and 2018. *Journal of Cleaner Production*, 202:1202–1219, 2018.

[16] Eugenia Gasparri, Angelo Lucchini, Gabriele Mantegazza, and Enrico Sergio Mazzucchelli. Construction management for tall clt buildings: From partial to total pre-

fabrication of façade elements. *Wood Material Science & Engineering*, 10(3):256–275, 2015.

[17] Edvard P.G. Bruun, Rafael Pastrana, Vittorio Paris, Alessandro Beghini, Attilio Pizzigoni, Stefana Parascho, and Sigrid Adriaenssens. Three cooperative robotic fabrication methods for the scaffold-free construction of a masonry arch. *Automation in Construction*, 129:103803, 2021.

[18] Adrian Long, Danny McPolin, James Kirkpatrick, Abhey Gupta, and David Courtenay. Flexiarch: From concept to practical applications. *The Structural Engineer: journal of the Institution of Structural Engineer*, 92(7):10–15, 2014.

[19] Philipp Eversmann, Fabio Gramazio, and Matthias Kohler. Robotic prefabrication of timber structures: towards automated large-scale spatial assembly. *Construction Robotics*, 1(1):49–60, 2017.

[20] Fabian Scheurer, Hanno Stehling, Franz Tschümperlin, and Martin Antemann. Design for assembly–digital prefabrication of complex timber structures. In *Proceedings of IASS Annual Symposia*, number 14, pages 1–7. International Association for Shell and Spatial Structures (IASS), 2013.

[21] Pablo Martinez, Michelle Livojevic, Purvish Jajal, Daniel Ryan Aldrich, Mohamed Al-Hussein, and Rafiq Ahmad. Simulation-driven design of wood framing support systems for off-site construction machinery. *Journal of Construction Engineering and Management*, 146(7):04020075, 2020.

[22] Ger Maas and Bert van Eekelen. The bollard—the lessons learned from an unusual example of off-site construction. *Automation in Construction*, 13(1):37–51, 2004. The best of ISARC 2002.

[23] Clinton Aigbavboa, Ayodeji Oke, and Yongama Thole. Sustainability of tilt-up construction method. *Procedia Manufacturing*, 7:518–522, 2017. International

Conference on Sustainable Materials Processing and Manufacturing, SMPM 2017, 23-25 January 2017, Kruger.

[24] Nathan C. Brown, Violetta Jusiega, and Caitlin T. Mueller. Implementing data-driven parametric building design with a flexible toolbox. *Automation in Construction*, 118:103252, 2020.

[25] Richard Garber. *BIM design: realising the creative potential of building information modelling*. John Wiley & Sons, 2014.

[26] Xianfei Yin, Hexu Liu, Yuan Chen, and Mohamed Al-Hussein. Building information modelling for off-site construction: Review and future directions. *Automation in Construction*, 101:72–91, 2019.

[27] Antonio Maria D'altri, Vasilis Sarhosis, Gabriele Milani, Jan Rots, Serena Cattari, Sergio Lagomarsino, Elio Sacco, Antonio Tralli, Giovanni Castellazzi, and Stefano De Miranda. Modeling strategies for the computational analysis of unreinforced masonry structures: review and classification. *Archives of computational methods in engineering*, 27:1153–1185, 2020.

[28] Dimitrios Loverdos, Vasilis Sarhosis, Efstathios Adamopoulos, and Anastasios Drougkas. An innovative image processing-based framework for the numerical modelling of cracked masonry structures. *Automation in Construction*, 125:103633, 2021.

[29] Dimitrios Loverdos and Vasilis Sarhosis. Image2dem: A geometrical digital twin generator for the detailed structural analysis of existing masonry infrastructure stock. *SoftwareX*, 22:101323, 2023.

[30] Marco Francesco Funari, Ameer Emad Hajjat, Maria Giovanna Masciotta, Daniel V. Oliveira, and Paulo B. Lourenço. A parametric scan-to-fem frame-

work for the digital twin generation of historic masonry structures. *Sustainability*, 13(19), 2021.

[31] Laura Niero, Carlo Pellegrino, Vasilis Sarhosis, and Paolo Zampieri. A methodology for the rapid and reliable assessment of existing masonry arch bridges containing defects. *Engineering Structures*, 339:120528, 2025.

[32] Dimitrios Loverdos and Vasilis Sarhosis. Geometrical digital twins of masonry structures for documentation and structural assessment using machine learning. *Engineering Structures*, 275:115256, 2023.

[33] Mohammad Pourfouladi, Natalia Pingaro, and Marco Valente. Polibrick plugin as a parametric tool for digital stereotomy modelling. *Computers & Structures*, 311:107722, 2025.

[34] Anjali Mehrotra and Matthew J. DeJong. A cad-interfaced dynamics-based tool for analysis of masonry collapse mechanisms. *Engineering Structures*, 172:833–849, 2018.

[35] Marco Francesco Funari, Luís Carlos Silva, Nathanael Savalle, and Paulo B Lourenço. A concurrent micro/macro fe-model optimized with a limit analysis tool for the assessment of dry-joint masonry structures. *International Journal for Multiscale Computational Engineering*, 20(5), 2022.

[36] Bowen Zeng and Yong Li. An improved method for statistics estimation of out-of-plane load resistance of masonry walls using design-code models and mechanics-based finite element models. *Engineering Structures*, 319:118725, 2024.

[37] Bjorn Ter Haar, Jacques Kruger, and Gideon van Zijl. Off-site construction with 3d concrete printing. *Automation in Construction*, 152:104906, 2023.

[38] Amin Alvanchi, Reza Azimi, SangHyun Lee, Simaan M. AbouRizk, and Paul Zubick. Off-site construction planning using discrete event simulation. *Journal of Architectural Engineering*, 18(2):114–122, 2012.

[39] Rafaela Sanches, Oya Mercan, and Brent Roberts. Experimental investigations of vertical post-tensioned connection for modular steel structures. *Engineering Structures*, 175:776–789, 2018.

[40] Yuxi Wei, Zhen Lei, and Sadiq Altaf. An off-site construction digital twin assessment framework using wood panelized construction as a case study. *Buildings*, 12(5), 2022.

[41] Matthew Gilbert, Kavinda Isuru Nanayakkara, Andrew Liew, Linwei He, Helen Fairclough, Serena Amodio, and James Rae-Smith. Use of off-site fabricated elements in the construction of modern unreinforced stone masonry buildings. In Gabriele Milani and Bahman Ghiassi, editors, *18th International Brick and Block Masonry Conference*, pages 765–774, Cham, 2025. Springer Nature Switzerland.

[42] Matthew Gilbert, Kavinda Isuru Nanayakkara, Andrew Liew, Linwei He, Helen Fairclough, Serena Amodio, James Rae-Smith, and Jian Zhang. Digitally engineered stone masonry building structures. In *Proceedings of the IASS 2024 Symposium*, 2024.

[43] Matthew Gilbert, Thomas Pritchard, and Colin Smith. *LimitState:RING Manual (Version 4.0) LimitState Ltd, Sheffield UK*, 2024. Computer software.

[44] Francesco Portioli, Claudia Casapulla, Matthew Gilbert, and Lucrezia Cascini. Limit analysis of 3d masonry block structures with non-associative frictional joints using cone programming. *Computers & Structures*, 143:108–121, 2014.

[45] Matthew Gilbert and Andrew Tyas. Layout optimization of large-scale pin-jointed frames. *Engineering computations*, 20(8):1044–1064, 2003.

[46] Linwei He, Matthew Gilbert, and Xingyi Song. A python script for adaptive layout optimization of trusses. *Structural and Multidisciplinary Optimization*, 60:835–847, 2019.

[47] Linwei He, Matthew Gilbert, Paul Shepherd, Jun Ye, Antiopi Koronaki, Helen E Fairclough, Buick Davison, Andy Tyas, Jacek Gondzio, and Alemseged G Weldeyesus. A new conceptual design optimization tool for frame structures. In *Proceedings of IASS Annual Symposia*, number 19, pages 1–8. International Association for Shell and Spatial Structures (IASS), 2018.

[48] Linwei He, Qingpeng Li, Matthew Gilbert, Paul Shepherd, Catherine Rankine, Thomas Pritchard, and Vincenzo Reale. Optimization-driven conceptual design of truss structures in a parametric modelling environment. In *Structures*, volume 37, pages 469–482. Elsevier, 2022.